Desalination and Water Treatment
www.deswater.com
doi: 10.1080/19443994.2014.983980

56 (2015) 1208–1216
October

Taylor & Francis
Taylor & Francis Group

Kinetic modeling of selenium (IV) adsorption for remediation of contaminated aquatic systems based on meso-scale experiments

Sevilay Haciyakupoglu[a,*], Esra Orucoglu[b], Ayse N. Esen[c], Sabriye Yusan[d], Sema Erenturk[a]

[a]*Energy Institute, Istanbul Technical University, 34469 Maslak, Istanbul, Turkey, Tel. +90 212 285 38 87; Fax: +90 212 285 38 84; email: haciyakup1@itu.edu.tr (S. Haciyakupoglu), Tel. +90 212 285 39 38; Fax: +90 212 285 38 84; email: erenturk@itu.edu.tr (S. Erenturk)*
[b]*Faculty of Mines, Istanbul Technical University, 34469 Maslak, Istanbul, Turkey, Tel. +90 212 285 61 83; Fax: +90 212 285 61 31; email: orucoglu@itu.edu.tr*
[c]*Faculty of Engineering, Istanbul Bilgi University, 34060 Eyup, Istanbul, Turkey, Tel. +90 212 311 72 41; Fax: +90 212 427 82 70; email: ayse.esen@bilgi.edu.tr*
[d]*Institute of Nuclear Sciences, Ege University, 35100 Bornova, Izmir, Turkey, Tel. +90 232 311 34 93; Fax: +90 232 311 34 33; email: sabriye.doyurum@ege.edu.tr*

Received 27 September 2013; Accepted 27 October 2014

ABSTRACT

The present study involves selenium (IV) adsorption onto organic pillared bentonite using batch experiments and kinetic modeling, at two different temperatures. selenium (IV) remediation in an aqueous environment, such as contaminated drinking water, groundwater, and industrial wastewater, is the aim of this study. The experimental data were tested with both surface reaction-based and diffusion-based kinetic models to clarify the controlling mechanism of the adsorption process from both microscopic and macroscopic point of view. Among all the investigated models, the most appropriate was the pseudo-second-order surface reaction-based kinetics model. The obtained results proved that the adsorption process at a selenium dioxide concentration of 300 mg L^{-1} is controlled by the diffusion rate of penetrated selenium (IV) into the reacted layer.

Keywords: Selenium; Adsorption; Remediation; Kinetic models; Diffusion coefficients

1. Introduction

Selenium (Se) is one of the essential trace elements, and has been studied often due to its complicated reactions. Although it plays an important role at low concentrations, it is poisonous at high ones due to the bioaccumulation property in the metabolism of living species [1–3]. Manmade factors, such as agricultural drain water, sewage sludge, fly ash from coal-fired power plants, oil refineries, and the mining of phosphates and metal ores, may facilitate the selenium release from the source and lead to aquatic environmental contamination. Fishes and plants from the

*Corresponding author.

Presented at the 4th International Conference on Environmental Management, Engineering, Planning and Economics (CEMEPE), 24–28 June 2013, Mykonos, Greece

aqueous environment uptake some water-soluble selenium particles, and in this way, selenium enters into the food chain [4]. Selenium occurs in four oxidation states as Se^{-2}, Se^{0}, Se^{+4}, and Se^{+6} in the environment, and can be found in the form of different ionic species, depending on the pH and Eh. Selenide (HSe^{-}) and elemental selenium (Se^{0}) in anaerobic zone, and selenite (SeO_3^{2-}) or selenate (SeO_4^{2-}) in oxidizing zone are the common species [5]. The investigations show that selenite uptake by living things is faster and greater than the selenate uptake in the aquatic environment [4].

Lime neutralization/softening, precipitation/coagulation, adsorption, membrane filtration, activated alumina, and reverse osmosis [6–12] are the most common treatment methods developed for the removal of selenium species. However, some disadvantages (poor elimination higher than 30 μg L^{-1} left in the solution, large volumes of mass sludge generation, high reagent cost, and time consuming removal process) make these methods less effective than the adsorption. Most of the research shows useful and cost-effective adsorption on adsorbents used for selenium removal by purifying drinking water and groundwater and by cleaning industrial wastewater [9–15]. In the study by Zelmanov and Semiat [15], iron-oxide based nanoparticles adsorbed 95–98% selenium from the solution and the residual selenium concentration reached less than 0.01 ppm, which is acceptable by water quality regulations.

Adsorption mechanisms can be explained by analyzing the kinetic parameters of an adsorption system. Furthermore, kinetic studies are important to understand the solute uptake that controls the residence time of adsorbate at the solid–solution interface [16,17]. Adsorption is a multi-step process including bulk diffusion, film diffusion, intraparticle diffusion, and adsorption of the solute on the surface [18–20]. Therefore, in many studies, surface reaction-based and diffusion-based kinetic models are used to explore macroscopic and microscopic processes realized between selenium species and solid phases [21–27].

This study highlights adsorption kinetic mechanisms of Se(IV) anions on organic pillared bentonite (OPBent) at 300 mg L^{-1} Se concentration and pH 3 were found to be the optimum adsorption conditions in our previous research [28]. In order to determine the kinetic parameters and to define which mechanism controls the Se(IV) sorption on OPBent under these conditions, microscopic (the homogeneous particle diffusion model (HPDM), the shell progressive model (SPM), and the Weber–Morris model) and macroscopic (Elovich model, pseudo-first-order and pseudo-second-order rate equations) kinetic models are applied to the batch data.

2. Materials and methods

2.1. Materials

Purified bentonite (Bent) obtained from Mining Engineering Department of Istanbul Technical University was modified with hexadecylpyridinium and Al-polyoxo cations. The modified bentonite called as OPBent was used as adsorbent in the experiments [29]. Particle size distribution of the adsorbent was measured with Fusion Frequency 9300H Model Particle Size Analyzer. Particle size of the adsorbent was found as 99 μm and that size was used in calculation.

The adsorbate solution was prepared with a radioactive SeO_2 compound that was produced by the irradiating of SeO_2 compound in the TRIGA MARK II nuclear research reactor, at Istanbul Technical University at 250 kW for 1 h.

2.2. Experimental procedures

The batch technique was used by a horizontal shaker bath for the adsorption kinetics studies. Based on our primary studies, the time-dependent adsorption was investigated for six different contact times (15, 30, 60, 120, 180, and 240 min) and the adsorbent/adsorbate ratio of 20 g L^{-1} at two different temperatures (20 and 50°C). The solid phase was separated from the liquid phase by centrifuging at 5,000 rpm for 5 min. The schematic view of the methodological process is given in Fig. 1.

Then, equal amounts of each initial adsorption solution and separated solution were transferred into polyethylene tubes for radioactivity measurements at high resolution gamma spectrometry. The gamma spectroscopy system was used to measure the relative activity of ^{75}Se, which was selected due to similar physical and chemical properties with ^{79}Se and a relatively short half-life of 119.779 d. The activity measurements were carried out with a GAMMA-X HPGe coaxial n-type germanium detector having 45.7% efficiency and 1.84 keV full width at half maximum for 1.3 MeV of ^{60}Co with an integrated digital gamma spectrometer (DSPEC jr 2.0). Gamma Vision-32 software program was used to detect the peak of ^{75}Se at 136 keV.

2.3. Selenium speciation

The relative distribution of different Se(IV) species in an aqueous solution as a function of pH at 300 mg L^{-1} selenium concentration was calculated and plotted (Fig. 2) using the equilibrium constants for the following reactions at ambient temperature [30,31]:

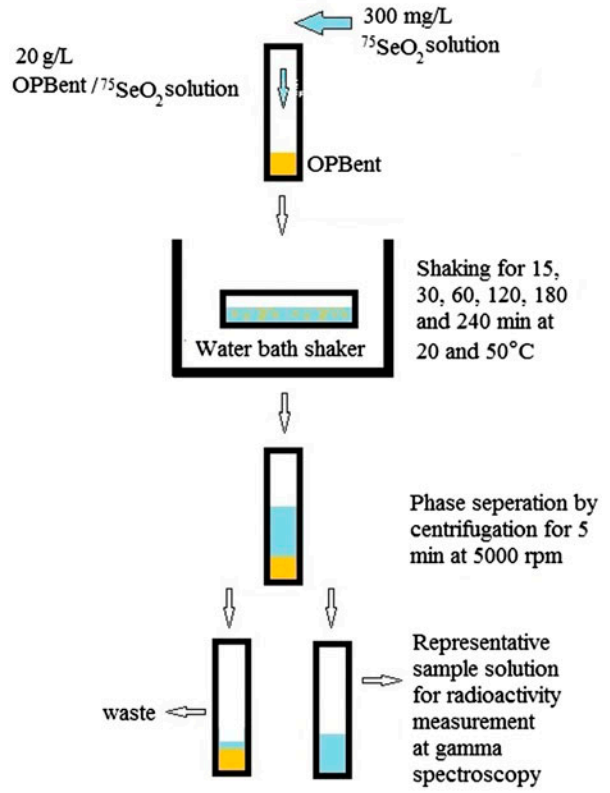

Fig. 1. Methodological process for Se(IV) adsorption on OPBent.

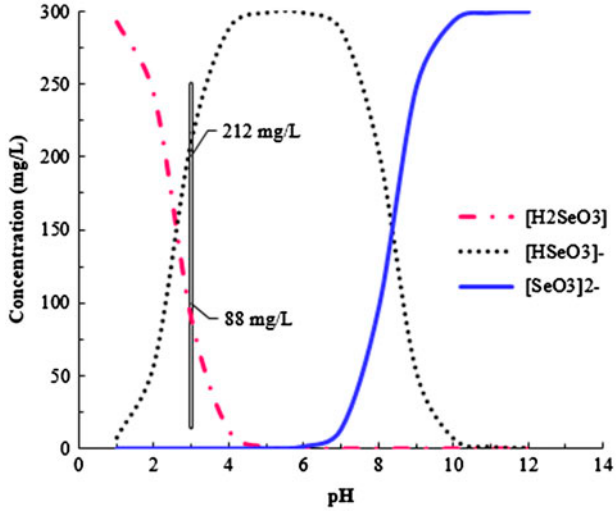

Fig. 2. Se(IV) species for concentration of 300 mg L^{-1}.

$$H_2SeO_3 \Longleftrightarrow HSeO_3^- + H^+ \quad pK_{a1} = 2.64 \tag{1}$$

$$HSeO_3^- \Longleftrightarrow SeO_3^{2-} + H^+ \quad pK_{a2} = 8.36 \tag{2}$$

Depending on pH, existing Se(IV) species are $HSeO_3^-$, H_2SeO_3, and SeO_3^{2-} complexes. $HSeO_3^-$ complex is the dominant species at 300 mg L^{-1} of selenium concentration and pH 3. Anion exchange reactions of Se(IV) with modified bentonite (OPBent) in the aqueous solution can be given as below [32]:

$$[OPBentOH] + [H]^+ + HSeO_3^- \Longleftrightarrow [OPBent\text{-}HSeO_3] + [H_2O] \tag{3}$$

2.4. Adsorption performance

The amount of adsorbed Se(IV) was estimated from the difference between the initial and final relative activities of ^{75}Se radioisotope. The experiments were performed in duplicate. The adsorption efficiency A of Se(IV) (%) in aqueous solution was computed as follows:

$$A = [(C_i - C_e)/C_j] \times 100 \tag{4}$$

where C_i is Se(IV) concentration of the initial solution (mg L^{-1}), C_e is Se(IV) concentration of the solution in equilibrium (mg L^{-1}).

2.5. Adsorption isotherms

Significant information about the distribution of the adsorbate between the liquid phase and solid phase at equilibrium can be obtained from adsorption isotherms [18,33]. In this study, most common models, Langmuir and Freundlich are used to describe the adsorption isotherms at different temperatures with the following two equations, respectively:

$$\frac{C_e}{q_e} = \frac{1}{K_L \cdot q_m} + \frac{C_e}{q_m} \tag{5}$$

and

$$\log\,(q_e) = \log\,(K_{FR}) + \frac{1}{n}\log\,(C_e) \tag{6}$$

In the equations C_e are the adsorbate concentrations at equilibrium and at beginning of adsorption. q_m is the maximum adsorption capacity, K_L is the Langmuir constant, K_F is the Freundlich constant, and $1/n$ is the heterogeneity factor. Dimensionless constant, R_L was calculated from the following equation using C_0 and K_L obtained from Langmuir isotherm:

$$R_L = \frac{1}{1 + K_L \cdot C_0} \quad (7)$$

The constants $0 < R_L < 1$ and $n > 0$ indicate the favorability of the adsorption for Langmuir and Freundlich models, respectively.

2.6. Adsorption kinetics

Adsorption is a multi-step process and generally described in three consecutive stages in the literature. In the first stage, molecules or ions from the substance of the solution move towards the exterior surface of adsorbent particles through a boundary layer (liquid film or external diffusion). In the second stage, molecules or ions diffuse through the interior pores of the adsorbent (intra particle or internal diffusion). In the last stage, adsorbent active sites adsorb ions or molecules by mechanisms of ion exchange, precipitation, complexion, or chelation. One of the steps which offer much greater resistance than the others can be considered as the rate-limiting step of the process [22,34].

2.6.1. Diffusion-based kinetics

In order to understand the kinetic process from a microscopic point of view, and to define which mechanism controls the adsorption process, two models are widely used for fitting experimental data: the homogeneous particle diffusion model (HPDM), and the shell progressive model (SPM) or the shrinking core model (SCM) [35–37].

The assumptions in the HPDM model are the diffusion of the adsorbates onto a homogeneous adsorbent surface, infinite dilution, and spherical adsorbent particle geometry. The diffusion rate controls the adsorption process by either the diffusion of ions through the liquid film surrounding the particle, or the diffusion of ions into the sorbent beads. The Nernst–Plank equation was used to establish the HPDM equations [35–37].

If the particle diffusion rate controls the adsorption process, the linearized equation is used to determine D_r ($m^2\,s^{-1}$) the particle diffusion coefficient in the solid phase:

$$-\ln[1 - X^2(t)] = 2(\pi^2 D_r / r^2)t \quad (8)$$

where X is the ratio of adsorbate amounts at time t (q_t) and equilibrium (q_e), and r (m) is the radius of the adsorbent particle.

If liquid film diffusion controls the rate of sorption, the following equation can be used:

$$-\ln\left[1 - \frac{q_t}{q_e}\right] = \left(\frac{3DC}{rC_r}\right) \cdot t \quad (9)$$

In this equation, C ($mol\,L^{-1}$) and C_r ($mol\,L^{-1}$) are the equilibrium concentrations of the ion in the solution and solid phase, respectively. D ($m^2\,s^{-1}$) is the diffusion coefficient in the liquid phase.

Another intraparticle diffusion model for the adsorption process was proved by Weber and Morris [35,38]. During their experiments, ions could diffuse into the pores of the adsorbent and could limit the rate of adsorption. This model can be described by:

$$q_t = k_p \cdot t^{0.5} \quad (10)$$

where q_t is the concentration of the adsorbed ion (mg g^{-1}) at time t, and k_p is the intraparticle diffusion rate constant for the intraparticle transport ($mg\,g^{-1}\,min^{-1}$). If the plot of q_t vs. $t^{0.5}$ exhibits a linear plot passing through the origin, the intraparticle diffusion would be the controlling step [35,38].

SPM or the SCM is based on the fluid-particle chemical reactions, and the reaction is considered to take place first at the outer surface of the particle. Then the region of the reaction goes into the solid, and the reacting particle shrinks during the reaction. The SPM assumptions are mentioned as follows: (a) Pore diffusivity is independent of concentration; (b) Adsorption isotherm is irreversible; (c) Pseudo-steady-state approximation is valid; (d) The driving force in both film and particle mass transfers is linear; and (e) Adsorbent particles are spherical [35–38]. In this model, the reactions occurring in the fluid–solid heterogeneous system generally had the following steps: diffusion of fluid reactant through the main body of the fluid layer to the surface of the solid, reaction of the fluid reactant with the solid on the surface of the solid, and the diffusion of the products through the film layer back to the bulk of the fluid. The slowest of these steps is considered the rate-determining step. If the process is the fluid-film diffusion control, the model is represented by:

$$X = \left(\frac{3C_A \cdot K_F}{z \cdot r \cdot C_s}\right) \cdot t \quad (11)$$

If the process is the product layer diffusion control, the model is represented by:

$$3 - 3(1 - X)^{2/3}2X = \left(\frac{6D_eC_A}{zr^2C_s}\right) \cdot t \quad (12)$$

If the process is the chemical reactions control, the model is represented by:

$$1 - (1 - X)^{1/3} = \left(\frac{k_sC_A}{r}\right) \cdot t \quad (13)$$

where C_A (mol L^{-1}) is the concentration of adsorbed ions in solution, C_s (mol L^{-1}) is the concentration of adsorbed ions in the remaining solution after the adsorption process, K_F (m s^{-1}) is the mass transfer coefficient of species through the liquid film, D_e (m^2 s^{-1}) is the diffusion coefficient through the reacted layer in the solid phase, k_s (m s^{-1}) is the reaction constant based on surface, r (m) is the average radius of adsorbent particles, and z is the stoichiometric coefficient, respectively [35].

2.6.2. Surface reaction-based kinetic models

In order to understand the adsorption process in terms of the order of the rate constant, the Se(IV) adsorption reaction kinetics of the adsorbent was studied by using the data obtained from the reaction time experiments. The pseudo-first-order model is the linearized form of the pseudo-first-order equation (Lagergren) [35] illustrated by:

$$\log(q_e - q_t) = \log q_e - \frac{k_1 t}{2.303} \quad (14)$$

where q_t and q_e (mg g^{-1}) are the amounts of the sorbed ions at equilibrium (mg g^{-1}) and at time t (min), respectively, and k_1 is the rate constant of the equation (min^{-1}).

The pseudo-second-order kinetic model is based on the experimental information from the solid phase adsorption, and was generally applied to the heterogeneous systems, where the adsorption mechanism is attributed to chemical adsorption. The model can be represented by the following equation:

$$\frac{t}{q_t} = \frac{1}{k^2.q_e^2} + \frac{t}{q_e} \quad (15)$$

The Elovich kinetic model equation was used in the chemical adsorption processes, and is suitable for systems with heterogeneous adsorbing surfaces [19]. The characteristics of the Elovich equation used for the analysis of adsorption kinetics by assuming a, b, $t \geq 1$ are expressed as:

$$q_t = \frac{1}{b \cdot \ln(ab)} + \frac{1}{b \cdot \ln(t)} \quad (16)$$

where q_t is the adsorption capacity at time t (mg g^{-1}), a and b are the Elovich parameters referring to the initial adsorption rate (mg g^{-1} min^{-1}) and the desorption constant (g mg^{-1}) during the experiment, respectively [34,35].

3. Results and discussion

3.1. Adsorption performance

The adsorption efficiency for different contact times and Se(IV) uptake by the adsorbent at various temperatures is given in Fig. 3.

The modified bentonite plots in Fig. 3 show a small increase in the adsorption process and reach nearly a constant value with 70% adsorption efficiency. The Pearson correlation coefficients (R values) for 20 and 50°C were obtained as 0.6737 and 0.8952, respectively.

3.2. Adsorption isotherms

Langmuir and Freundlich isotherm parameters were obtained from the experimental adsorption data using the plots of C_e/q_e vs. C_e and log (q_e) vs. log (C_e). The results of Langmuir ($0 < R_L < 1$) and Freundlich ($n > 1$) isotherms (Table 1) show that adsorption is favorable and at higher selenium concentrations the adsorption is practically irreversible (R_L approach to zero) as defined in the literature [39,40]. The value of Freundlich constants indicates heterogeneity of the OPBent surface and high affinity of OPBent for selenium.

From the correlation coefficients it can be concluded that the Freundlich model fitted the experimental results better than the Langmuir model.

3.3. Kinetic experiments

As seen in Fig. 4 and Table 2, Weber–Morris model plots did not pass through the origin, and only adsorption experiments at 50°C gives acceptable correlation coefficient. This indicates that intraparticle diffusion is effective at 50°C, but it is not the only rate-controlling step as described in many studies [27,35].

Results given in Tables 3–4 indicate that temperature increase provides diffusion for both models.

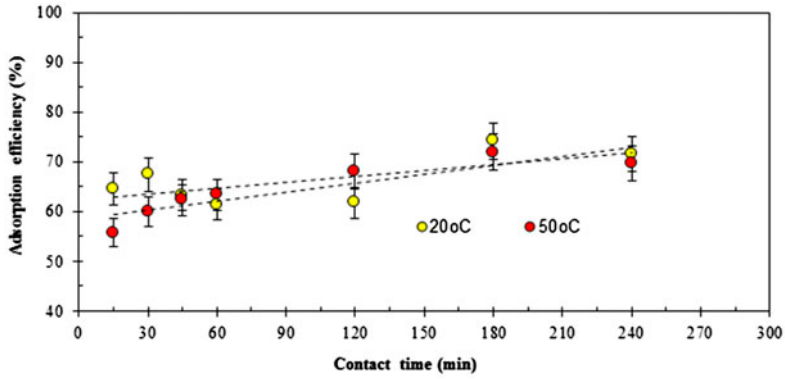

Fig. 3. Effect of contact time on adsorption efficiency.

Table 1
Adsorption isotherm parameters

Isotherm model	Langmuir	Freundlich
Constants	$q_m = 0.0001$ μg g^{-1} $K_L = 0.0244$ mL μg^{-1} $R_L = 0.291$–0.0394[a] $R^2 = 0.9747$	$K_{FR} = 25$ (μg g^{-1}) (L μg^{-1})$^{1/n}$ $n = 3.6$ $R^2 = 0.9779$

[a]R_L changes between 0.291 and 0.0394 for minimum and maximum concentration range.

Table 2
Linear regression analysis of Weber–Morris model

Temp (°C)	k_p (mg g^{-1})	R^2
20	0.1053	0.3677
50	0.1907	0.9013

Table 3
Linear regression analysis of HPDM functions

	In solid phase		In liquid phase	
Temp (°C)	D_r (m^2 s^{-1})	R^2	D (m s^{-1})	R^2
20	7.94×10^{-14}	0.5426	5.42×10^{-8}	0.5330
50	9.93×10^{-14}	0.9399	4.14×10^{-8}	0.9343

It is found that at 20°C the HPDM and SPM could not fit experimental data reasonably, but at 50°C both models fitted the results better than at 20°C. The magnitude of D_r of HPDM is the slowest process for Se (IV) adsorption. Therefore, it may be concluded that the diffusion of Se(IV) anions through the OPBent particle is the slowest process and hence it is the rate-determining step, at 50°C. The Se(IV) ions would have to diffuse across a surface liquid film, diffuse through the OPBent particle, and finally react with the hexadecyl pyridiniumchloride modifier in the OPBent particle.

This result is also in accordance with the studies where it is pointed out that the kinetic process of adsorption is always controlled by liquid film diffusion or intraparticle diffusion, i.e. one of the processes should be the rate-limiting step [27]. Real world results suggest that OPBent is effective in removing Se

Table 4
Linear regression analysis of SPM functions

	Film diffusion		Layer diffusion		Chemical reactions	
Temp (°C)	K_F (m s^{-1})	R^2	D_e (m^2 s^{-1})	R^2	k_s (m s^{-1})	R^2
20	1.31×10^{-10}	0.3397	1.30×10^{-14}	0.4571	5.12×10^{-7}	0.4690
50	1.29×10^{-10}	0.7732	2.52×10^{-11}	0.8823	1.02×10^{-6}	0.8904

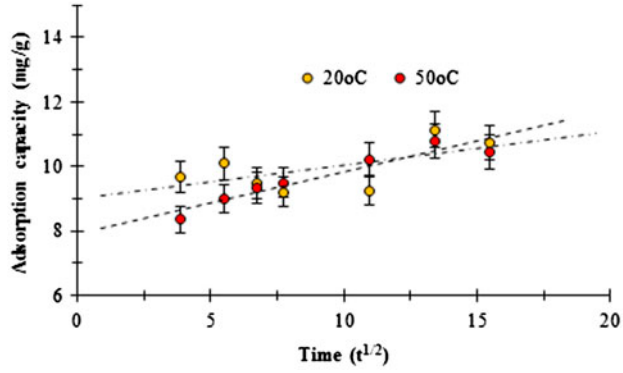

Fig. 4. Weber–Morris plots for adsorption of Se(IV) on OPBent.

(IV) anions from contaminated water by different mechanisms.

The calculated reaction kinetic parameters given in Table 5 show that the pseudo-second-order kinetic model is the most appropriate model under the experimental conditions. Although the Elovich kinetic model fits the experimental data at 50℃ adequately with a high correlation coefficient (>0.95), it does not fit the data at 20℃ as revealed by the low correlation coefficient.

The mechanism of the adsorption kinetic process can be clarified with pseudo-second-order rate equation, because chemical bonding among selenite anions and functional groups on OPBent may be responsible for the adsorption. The Elovich equation reported a good agreement at 50℃ and confirms the chemical adsorption process at a high temperature.

Table 5
Adsorption kinetic parameters for experimental conditions

Model	20℃	50℃
Pseudo-first-order model		
k_1 (min^{-1})	0.0053	0.0085
q_e ($mg\,g^{-1}$)	1.912	2.227
R^2	0.5330	0.9343
Pseudo-second-order kinetic model		
k_2 ($g\,mg^{-1}\,min^{-1}$)	0.013	0.015
q_e ($mg\,g^{-1}$)	11.00	10.85
R^2	0.9910	0.9990
Experimental q_e ($mg\,g^{-1}$)	11.12	10.79
Elovich kinetic model		
a ($mg\,g^{-1}\,min^{-1}$)	1.31×10^9	1.14×10^3
b ($g\,mg^{-1}$)	2.632	1.181
R^2	0.2590	0.9599

4. Conclusions

Some kinetic models were used to evaluate the experimental data and to determine the mechanism Se (IV) adsorption process. Kinetic studies confirmed that more than 60% of Se(IV) removal took place within the first 15 min of contact time. By modeling Se(IV) adsorption for the remediation of contaminated aquatic systems, it was found that the diffusion of Se(IV) anions $HSeO_3^-$ through the OPBent particle was the rate-determining step at 50℃, and that intraparticle diffusion is also involved in the adsorption process. The adsorption kinetics described by the relationship between the contact time and the Se(IV) uptake by the adsorbent for temperatures of 20 and 50℃ showed that the pseudo-second-order model is the most appropriate model for both temperatures. Considering these results, modified bentonites can also be used in the removal of other anionic species in polluted aqueous media. Further studies are in progress, and understanding the kinetics of selenium adsorption on modified bentonites may contribute to other Se(IV) pollution remediation studies.

Symbols

A — adsorption efficiency
a — Elovich parameter referring to the initial adsorption rate
b — Elovich parameter referring to desorption constant
C — equilibrium concentration of sorbed ion in the solution
C_A — the concentration of sorbed ion in the solution
C_e — sorbed ion concentration of the solution at equilibrium
C_i — sorbed ion concentration of the initial solution
C_r — equilibrium concentration of the sorbed ion in the solid phase
C_s — concentration of sorbed ions remained solution after the adsorption process
D_e — diffusion coefficient through the reacted layer in the solid phase
D_r — particle diffusion coefficient
k_1 — rate constant
K_F — mass transfer coefficient of species through the liquid film
K_{FR} — Freundlich constant represent adsorption capacity
K_L — Langmuir constant related to the affinity of binding sites
k_p — intraparticle diffusion rate constant for the intraparticle transport
k_s — reaction constant based on surface
n — Freundlich constant representing the adsorption strength

pKa — acid dissociation constant at logarithmic scale
q_e — adsorption capacity at equilibrium
q_m — maximum monolayer adsorption capacity
q_t — adsorption capacity or concentration of the sorbed ion at time t
r — average radius of adsorbent particle
r — radius of the adsorbent particle
R_L — dimensionless Langmuir constant
X — fraction attainment of equilibrium
z — stoichiometric coefficient

References

[1] J.M. Pacyna, E. Pacyna, An assessment of global and regional emissions of trace metals to the atmosphere from anthropogenic sources worldwide, Environ. Rev. 9 (2002) 269–298.
[2] M. Lenz, P.N.L. Lens, The essential Toxin: The changing perception of selenium in environmental sciences, Sci. Total Environ. 407 (2009) 3620–3633.
[3] EPA/600/R-01/077, Selenium Treatment/Removal Alternatives Demonstration Project, Mine Waste Technology Program Activity III, Project 20, 2001.
[4] S.J. Hamilton, Review of selenium toxicity in the aquatic food chain, Sci. Total Environ. 326 (2004) 1–31.
[5] T. Sandy, C. DiSante, Review of Available Technologies for the Removal of Selenium from Water, Final Report Prepared for North American Metals Council, CH2M Hill Inc., 2010.
[6] V. Mavrov, S. Stamenov, E. Todorova, H. Chmiel, T. Erwe, New hybrid electrocoagulation membrane process for removing selenium from industrial wastewater, Desalination 201 (1–3) (2006) 290–296.
[7] S. Kongsri, K. Janpradit, K. Buapa, S. Techawongstien, S. Chanthai, Nanocrystalline hydroxyapatite from fish scale waste: Preparation, characterization and application for selenium adsorption in aqueous solution, Chem. Eng. J. 215–216 (2013) 522–532.
[8] A.D. Lemly, Aquatic selenium pollution is a global environmental safety issue, Ecotox. Environ. Safe. 59 (2004) 44–56.
[9] N. Geoffroy, G.P. Demopoulos, The elimination of selenium(IV) from aqueous solution by precipitation with sodium sulphide, J. Hazard. Mater. 185 (2011) 148–154.
[10] N. Bleiman, Y.G. Mishael, Selenium removal from drinking water by adsorption to chitosan–clay composites and oxides: Batch and columns tests, J. Hazard. Mater. 183 (2010) 590–595.
[11] J. Muller, A. Abdelouas, S. Ribet, B. Grambow, Sorption of selenite in a multi-component system using the "dialysis membrane" method, Appl. Geochem. 27 (2012) 2524–2532.
[12] D. Low, A. Hamood, T. Reid, T. Mosley, P. Tran, L. Song, A. Morse, Attachment of selenium to a reverse osmosis membrane to inhibit biofilm formation of S-aureus, J. Membr. Sci. 378 (2011) 171–178.
[13] U.K. Saha, C. Liu, L.M. Kozak, P.M. Huang, Kinetics of selenite adsorption on hydroxyaluminum- and hydroxyaluminosilicate–montmorillonite complexes, Soil Sci. Soc. Am. J. 68 (2004) 1197–1209.
[14] R. Dobrowolski, M. Otto, Preparation and evaluation of Fe-loaded activated carbon for enrichment of selenium for analytical and environmental purposes, Chemosphere 90 (2013) 683–690.
[15] G. Zelmanov, R. Semiat, Selenium removal from water and its recovery using iron (Fe^{3+}) oxide/hydroxide-based nanoparticles sol (NanoFe) as an adsorbent, Sep. Purif. Technol. 103 (2013) 167–172.
[16] E. Demirbas, M. Kobya, E. Senturk, T. Ozkan, Adsorption kinetics for the removal of chromium (VI) from aqueous solutions on the activated carbons prepared from agricultural wastes, Water SA 30 (2004) 533–540.
[17] Y.S. Ho, Citation review of Lagergren kinetic rate equation on adsorption reactions, Scientometrics 59 (2004) 171–177.
[18] C.Y. Kuo, C.H. Wu, J.Y. Wu, Adsorption of direct dyes from aqueous solutions by carbon nanotubes: Determination of equilibrium, kinetics and thermodynamics parameters, J. Colloid Interface Sci. 327 (2008) 308–315.
[19] W. Plazinski, W. Rudzinski, A. Plazinska, Theoretical models of sorption kinetics including a surface reaction mechanism: A review, Adv. Colloid Interface Sci. 152 (2009) 2–13.
[20] A. Milutinović-Nikolić, D. Maksinb, N. Jović-Jovičić, M. Mirković, D. Stanković, Z. Mojović, P. Banković, Removal of 99Tc(VII) by organo-modified bentonite, Appl. Clay Sci. 95 (2014) 294–302.
[21] M. Caetano, C. Valderrama, A. Farran, J.L. Cortina, Phenol removal from aqueous solution by adsorption and ion exchange mechanisms onto polymeric resins, J. Colloid Interface Sci. 338 (2009) 402–409.
[22] V.J. Inglezakis, S.G. Poulopoulos, Adsorption, Ion Exchange, and Catalysis, Elsevier Science, Amsterdam, 2006.
[23] M. Belhachemi, F. Addoun, Adsorption of congo red onto activated carbons having different surface properties: studies of kinetics and adsorption equilibrium, Desalin. Water Treat. 37 (2012) 122–129.
[24] Z. Hua, N. Wang, J. Tanb, J. Chena, W. Zhong, Kinetic and equilibrium of cefradine adsorption onto peanut husk, Desalin. Water Treat. 37 (2012) 160–168.
[25] P. Chakravarty, D.C. Deka, N.S. Sarma, H.P. Sarma, Removal of copper(II) from wastewater by heartwood powder of *Areca catechu*: Kinetic and equilibrium studies, Desalin. Water Treat. 40 (2012) 194–203.
[26] R.P. Jena, S. De, J.K. Basu, A generalized shrinking core model applied to batch adsorption, Chem. Eng. J. 95 (2003) 143–154.
[27] H. Qiu, L. Lv, B.C. Pan, Q.J. Zhang, W.M. Zhang, Q.X. Zhang, Critical review in adsorption kinetic models, Zhejiang Univ. Sci A. 10(5) (2009) 716–724.
[28] S. Haciyakupoglu, S. Akyıl Erenturk, N. Karatepe, A.B. Tugrul, A.F. Baytas, N. Altinsoy, N. Baydogan, B. Buyuk, E. Demir, Remediation Investigation of Selenium in Aqueous Environment with using Activated Carbon, Global Conference on Global Warming 2012, Istanbul, Turkey, 08–12 July, 2012.
[29] E. Orucoglu, Modification of Reşadiye bentonite by using organic and inorganic cations and investigation of ^{75}Se radioisotope adsorption on the modified products, Istanbul Technical University, PhD Thesis, 2011.

[30] T. Wang, J. Wang, J.G. Burken, H. Ban, K. Ladwig, The leaching characteristics of selenium from coal fly ashes, J. Environ. Qual. 36 (2007) 1784–1792.
[31] Å. Olin, B. Noläng, E.G. Osadchii, L. Öhman, E. Rosen, Chemical Thermodynamics of Selenium. OECD Nuclear Energy Agency, Data Bank, Issy-Les-Moulineaux, 2005.
[32] T. Missana, U. Alonso, M. García-Gutiérrez, Experimental study and modeling of selenite sorption onto illite and smectite clays, J. Colloid Interface Sci. 334 (2009) 132–138.
[33] H. Fan, L. Zhou, X. Jiang, Q. Huang, W. Lang, Adsorption of Cu^{2+} and methylene blue on dodecyl sulfobetaine surfactant-modified montmorillonite, Appl. Clay Sci. 95 (2014) 150–158.
[34] Y. Xie, K.J. Jing, Y. Lu, Kinetics, equilibrium and thermodynamic studies of l-tryptophan adsorption using a cation exchange resin, Chem. Eng. J. 171 (2011) 1227–1233.
[35] C. Valderrama, J.I. Barios, M. Caetano, A. Farran, J.L. Cortina, Kinetic evaluation of phenol/aniline mixtures adsorption from aqueous solutions onto activated carbon and hypercrosslinked polymeric resin (MN200), React. Funct. Polym. 70 (2010) 142–150.
[36] C. Valderrama, X. Gamisans, X. de las Heras, A. Farr´an, J.L. Cortina, Sorption kinetics of polycyclic aromatic hydrocarbons removal using granular activated carbon: Intraparticle diffusion coefficients, J. Hazard. Mater. 157 (2008) 386–396.
[37] J.L. Cortina, R. Arad-Yellin, N. Miralles, A.M. Sastre, A. Warshawsky, Kinetics studies on heavy metal ions extraction by Amberlite XAD2 impregnated resins containing a bifunctional organophosphorous extractant, React. Funct. Polym. 38 (1998) 269–278.
[38] A. Omri, M. Benzina, W. Trabelsi, N. Ammar, Adsorptive removal of humic acid on activated carbon prepared from almond shell: Approach for the treatment of industrial phosphoric acid solution, Desalin. Water Treat. 52 (2014) 2241–2252.
[39] P. Baskaralingam, M. Pulikesi, D. Elango, V. Ramamurthi, S. Sivanesan, Adsorption of acid dye onto organobentonite, J. Hazard. Mater. B 128 (2006) 138–144.
[40] B.H. Hameed, A.A. Ahmad, N. Aziz, Isotherms, kinetics and thermodynamics of acid dye adsorption on activated palm ash, Chem. Eng. J. 133 (2007) 195–203.